Prediction of the development of new coronary atherosclerotic plaques with radiomics

Lee, S.E.; Hong, Y.; Jung, J.; Sung, J.M.; Andreini, D.; Al-Mallah, M.H.; ... ; Chang, H.J.

Journal of Cardiovascular Computed Tomography 18 (2024) 274–280

Contents lists available at ScienceDirect

Journal of Cardiovascular Computed Tomography

journal homepage: www.JournalofCardiovascularCT.com

Research paper

Prediction of the development of new coronary atherosclerotic plaques with radiomics

Sang-Eun Lee [a,b,1], Youngtaek Hong [b,1], Jongsoo Hong [c], Juyeong Jung [d], Ji Min Sung [b], Daniele Andreini [e,f], Mouaz H. Al-Mallah [g], Matthew J. Budoff [h], Filippo Cademartiri [i], Kavitha Chinnaiyan [j], Jung Hyun Choi [k], Eun Ju Chun [l], Edoardo Conte [m], Ilan Gottlieb [n], Martin Hadamitzky [o], Yong Jin Kim [p], Byoung Kwon Lee [q], Jonathon A. Leipsic [r], Erica Maffei [s], Hugo Marques [t], Pedro de Araújo Gonçalves [t], Gianluca Pontone [m,u], Sanghoon Shin [a], Peter H. Stone [v], Habib Samady [w], Renu Virmani [x], Jagat Narula [y], Leslee J. Shaw [z], Jeroen J. Bax [aa], Fay Y. Lin [z], James K. Min [ab], Hyuk-Jae Chang [b,ac,*]

[a] Division of Cardiology, Department of Internal Medicine, College of Medicine, Ewha Womans University, Seoul, South Korea
[b] CONNECT-AI Research Center, Yonsei University College of Medicine, Seoul, South Korea
[c] Division of Biostatistics, Department of Biomedical Systems Informatics, Yonsei University College of Medicine, Seoul, South Korea
[d] Graduate School of Medical Science, Brain Korea 21 Project, Yonsei University College of Medicine, Seoul, South Korea
[e] IRCCS Ospedale Galeazzi Sant'Ambrogio, Milan, Italy
[f] Department of Biomedical and Clinical Sciences, University of Milan, Milan, Italy
[g] Houston Methodist DeBakey Heart & Vascular Center, Houston Methodist Hospital, Houston, TX, USA
[h] Department of Medicine, Lundquist Institute at Harbor-UCLA, Torrance, CA, USA
[i] Department of Radiology, Fondazione Monasterio, Pisa, Italy
[j] Department of Cardiology, William Beaumont Hospital, Royal Oak, MI, USA
[k] Pusan University Hospital, Busan, South Korea
[l] Seoul National University Bundang Hospital, Seongnam, South Korea
[m] Centro Cardiologico Monzino IRCCS, Milan, Italy
[n] Department of Radiology, Casa de Saude São Jose, Rio de Janeiro, Brazil
[o] Department of Radiology and Nuclear Medicine, German Heart Center Munich, Munich, Germany
[p] Department of Internal Medicine, Seoul National University College of Medicine, Cardiovascular Center, Seoul National University Hospital, Seoul, South Korea
[q] Gangnam Severance Hospital, Yonsei University College of Medicine, Seoul, South Korea
[r] Department of Medicine and Radiology, University of British Columbia, Vancouver, BC, Canada
[s] IRCCS SYNLAB SDN, Naples, Italy
[t] UNICA, Unit of Cardiovascular Imaging, Hospital da Luz, Lisbon, Portugal
[u] Department of Biomedical, Dental and Surgical Sciences, University of Milan, Milan, Italy
[v] Division of Cardiovascular Medicine, Brigham and Women's Hospital, Boston, MA, USA
[w] Georgia Heart Institute, Northeast Georgia Health System, Gainesville, GA, USA
[x] Department of Pathology, CVPath Institute, Gaithersburg, MD, USA
[y] University of Texas Health Houston, Houston, TX, USA
[z] Icahn School of Medicine at Mount Sinai, New York, NY, USA
[aa] Department of Cardiology, Leiden University Medical Center, Leiden, The Netherlands
[ab] Cleerly, Inc, New York, NY, USA
[ac] Division of Cardiology, Severance Cardiovascular Hospital, Yonsei University College of Medicine, Yonsei University Health System, Seoul, South Korea

Abbreviations: ACS, acute coronary syndrome; CAD, coronary artery disease; CCC, concordance correlation coefficient; CCTA, coronary computed tomography angiography; CI, confidence interval; IDI, integrated discrimination improvement; NRI, net reclassification improvement; PV, plaque volume.

* Corresponding author. Division of Cardiology, Severance Cardiovascular Hospital, Yonsei University College of Medicine, Yonsei University Health System, 50-1 Yonsei-ro, Seodaemun-gu, Seoul 03722, South Korea.
E-mail address: hjchang@yuhs.ac (H.-J. Chang).

[1] These authors contributed equally.

https://doi.org/10.1016/j.jcct.2024.02.003
Received 20 November 2023; Received in revised form 1 February 2024; Accepted 12 February 2024
Available online 19 February 2024

ARTICLE INFO

Keywords:
Coronary artery disease
Coronary artery atherosclerosis
Coronary computed tomography angiography
Radiomics

ABSTRACT

Background: Radiomics is expected to identify imaging features beyond the human eye. We investigated whether radiomics can identify coronary segments that will develop new atherosclerotic plaques on coronary computed tomography angiography (CCTA).

Methods: From a prospective multinational registry of patients with serial CCTA studies at ≥ 2-year intervals, segments without identifiable coronary plaque at baseline were selected and radiomic features were extracted. Cox models using clinical risk factors (**Model 1**), radiomic features (**Model 2**) and both clinical risk factors and radiomic features (**Model 3**) were constructed to predict the development of a coronary plaque, defined as total PV ≥ 1 mm^3, at follow-up CCTA in each segment.

Results: In total, 9583 normal coronary segments were identified from 1162 patients (60.3 ± 9.2 years, 55.7% male) and divided 8:2 into training and test sets. At follow-up CCTA, 9.8% of the segments developed new coronary plaque. The predictive power of **Models 1** and **2** was not different in both the training and test sets (C-index [95% confidence interval (CI)] of **Model 1** vs. **Model 2**: 0.701 [0.690–0.712] vs. 0.699 [0.0.688–0.710] and 0.696 [0.671–0.725] vs. 0.0.691 [0.667–0.715], respectively, all $p > 0.05$). The addition of radiomic features to clinical risk factors improved the predictive power of the Cox model in both the training and test sets (C-index [95% CI] of **Model 3**: 0.772 [0.762–0.781] and 0.767 [0.751–0.787], respectively, all $p < 00.0001$ compared to **Models 1** and **2**).

Conclusion: Radiomic features can improve the identification of segments that would develop new coronary atherosclerotic plaque.

Clinical Trial Registration: ClinicalTrials.gov NCT0280341.

1. Introduction

Coronary artery disease (CAD) remains the leading cause of mortality.[1] Therefore, early detection of CAD is essential to initiate preventive measures and improve outcomes. In this regard, noninvasive imaging modalities that allow direct visualization of coronary atherosclerosis have been incorporated into recent clinical guidelines,[2–4] and coronary computed tomography angiography (CCTA) has been proposed as a first-line test in patients with stable chest pain based on its reliability and accuracy in assessing luminal stenosis.[5]

In recent studies quantitatively evaluating CCTA, the presence of an atherosclerotic plaque is usually defined as any tissue ≥1 mm^3 within or adjacent to the lumen that can be distinguished from the surrounding structures.[6,7] The threshold of 1 mm^3 is mainly due to the limitation of spatial resolution, and the naked eye cannot detect plaques small enough to be indistinguishable from adjacent structures. However, there may be more information hidden beneath the images.

Recent technical developments in artificial intelligence have introduced the concept of radiomics.[8–10] Radiomics uses data characterization algorithms to extract vast amounts of quantitative information that are invisible to the naked eye. These radiomic features could potentially reveal tumoral patterns and informative multidimensional characteristics. By identifying those at risk using radiomics, selection of patients at higher risk would benefit from more aggressive preventive measures that would improve clinical outcomes.

Therefore, we evaluated whether the radiomic features can identify normal coronary segments that will develop new coronary atherosclerotic plaques at follow-up in a large multinational, multicenter serial CCTA dataset.

2. Methods

2.1. Study design and population

The Progression of AtheRosclerotic PlAque DetermIned by Computed TomoGraphic Angiography Imaging (PARADIGM) study is a dynamic multinational observational registry that prospectively collected clinical, procedural, and follow-up data on 2252 consecutive patients who underwent clinically indicated serial CCTAs. The inter-scan interval was ≥2 years, and patient data was collected from 13 sites in seven countries between 2003 and 2015.[11] The study protocol was approved by the institutional review boards of all participating centers.

For the current analysis, patients were excluded for the following reasons; (1) 492 patients with non-interpretable CCTA on 0.5 mm analysis, (2) 231 patients with history of revascularization before baseline CCTA, (3) 184 patients with clinical event during the interscan interval, (4) 86 patients with poor image quality of baseline CCTA, (5) 69 patients with CCTA images with failed to extract radiomic features, and (6) 28 patients with every segments with identifiable coronary atherosclerotic plaques at baseline CCTA. At the end, 9583 segments without visually identifiable coronary plaque at baseline CCTA were identified from 1162 patients and included for the final analysis. Patients were randomly divided into the training set (929 patients with 7674 segments) and the test set (233 patients with 1909 segments) in 8:2 manner. (Fig. 1).

2.2. Coronary computed tomography angiography analysis protocol

Acquisition and analysis of CCTAs were performed in accordance with the guidelines provided by the Society of Cardiovascular Computed Tomography.[6,12] CCTA datasets were analyzed at a core laboratory by Level III experienced readers using semi-automated plaque analysis software (QAngioCT Research Edition v2.1.9.1; Medis Medical Imaging, Leiden, the Netherlands) with manual correction as described previously.[13,14]

Briefly, all coronary segments with diameters ≥2 mm were evaluated for every coronary artery and its branches, using a modified 17-segment American Heart Association model.[6,7] For serial comparisons of CCTAs, coronary segments were co-registered between the baseline and follow-up CCTAs evaluations using fiduciary landmarks, including the distance from the ostium and the branch vessels. The length of segment and total plaque volume (PV) (mm^3) was determined for each segment. The total PV of each segment was summed to generate a patient-level total PV,[15] and normal CCTA was defined as patients with a per-patient total PV of 0 mm^3.

For the current analysis, only segments without any identifiable coronary plaques at baseline CCTA were included. The presence or development of visually identifiable coronary atherosclerotic plaque within a segment was defined as any tissue ≥1 mm^3 within, or adjacent to, the lumen that could be distinguished from the surrounding pericardial tissue, epicardial fat, or the lumen, and identified in ≥2 planes.[6,7]

To minimize the potential error in the quantitative comparison of serial CCTAs, the gap between the vessel wall and the lumen wall was ignored in the analysis of the PARADIGM dataset.[11,16,17] As a result, the selected normal coronary segments contain information from both the vessel wall and the lumen itself.

2.3. Extraction of radiomic features

An open-source Python package Pyradiomics was used to extract the radiomic features.[18]

The basic set of 91 radiomic features consisted of 18 first-order statistical features, 22 co-occurrence matrix, 16 Gy level run length matrix, 16 Gy level size zone matrix, 14 Gy level dependence matrix, and 5 neighboring gray level difference matrix-based texture features. After applying 8 wavelet filters, the same set of 91 radiomic features was extracted repeatedly for each wavelet filter. As a result, a total of 819 radiomic features were extracted from each identified coronary segment. Since the entire vessel segment was included, ignoring the gap between the vessel wall and the lumen wall, no shape features were extracted.

2.4. Feature selection

To ensure the reproducibility and to limit the variability of the radiomic features,[9] the concordance correlation coefficient (CCC) was calculated.[19] For inter-observer agreement, 155 randomly selected segments were analyzed by four imaging cardiologists, and 132 features with CCC <0.85 were excluded from the 819 radiomic features. For intra-observer agreement, two imaging cardiologists each randomly selected 54 segments and analyzed these segments twice. Among the 819 radiomic features, 24 features with a CCC less than 0.85 were excluded. Finally, 683 radiomic features with both inter- and intra-observer agreement greater than 0.85 were included in the next step.

The Boruta and XGboost algorithms were used to further select the radiomic features.[20] The Boruta algorithm was used to select the top-ranked features associated with coronary atherosclerotic plaque development.[21] The importance ranking for each variable was calculated with the Boruta algorithm, and the top-ranked features (rank 1) were selected as candidates for modeling. The XGBoost algorithm, which combines multiple weak classifiers to produce a single strong classifier, was used to select the final features and construct a Cox regression model.[22,23] XGBoost ranks features by "gain," which represents the fractional contribution of each feature to the model based on the total gain of the splits of that feature. Features with no information gain were excluded.

2.5. Statistical analysis & Cox modeling

Categorical variables are presented as absolute counts and percentages, and continuous variables are expressed as means ± standard deviation or medians [interquartile range] as appropriate. Differences between categorical variables were analyzed using the chi-square test or Fisher's exact test, as appropriate, while differences between continuous variables were assessed using the Student's t-test.

Multivariable Cox regression models predicting the development of a coronary plaque in a segment were constructed using cluster analysis to account for the effects of common clinical factors in clustered segments within a single patient. **Model 1** was adjusted only for clinical variables including age, male sex, body-mass index, systolic blood pressure, smoking history, hypertension, diabetes mellitus, family history of CAD, low-density lipoprotein cholesterol level, medication use including statins, antiplatelets, and beta-blockers, luminal attenuation, and the total PV of the given patient at baseline. **Model 2** was constructed using only radiomic features, and **Model 3** included both the clinical variables and the selected radiomic features. The predictive performance of each model was assessed using Harrell's C-index (area under the receiver operating characteristic curve), and differences in predictive performance between models were tested using a nonparametric method.[24] A standard bootstrap method was applied to generate the corresponding confidence intervals (CI) for this estimate.[25] The integrated discrimination improvement (IDI) and the net reclassification improvement (NRI) were calculated to compare the performance of **Model 1** vs. **Model 2** and **Model 1** vs. **Model 3** in the training set.[26]

A two-tailed p value < 0.05 was considered statistically significant. All analyses were performed using SAS version 9.4 (SAS Institute Inc., Cary, NC, USA) and R 3.3.0 (R Development Core Team, 2016).

3. Results

3.1. Study population and baseline characteristics

The study population consisted of 1162 patients (60.3 ± 9.2 years old, 55.7% male) with 9583 coronary segments. Hypertension was presented in 51.6% of patients, and diabetes mellitus was noted in 19.9%. Statin

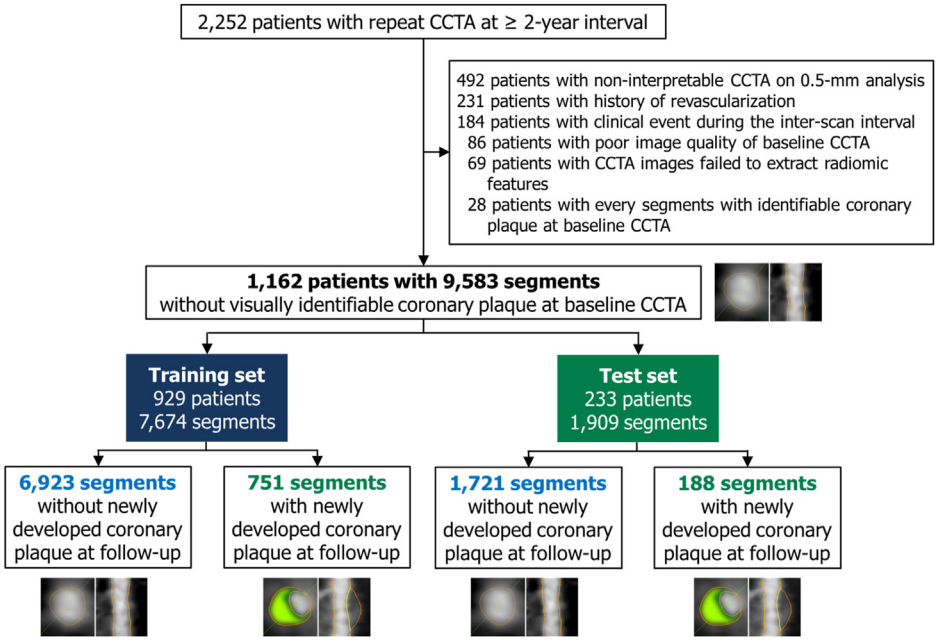

Fig. 1. CONSORT diagram.
CCTA, coronary computed tomography angiography.

was used in 53.8% of the study population. The mean interval between CCTAs was 3.8 ± 1.5 years. When patients were divided into training set and test set in 8:2 manner, there were no differences between patients in training set and test set in clinical characteristics (Table 1). Of the total patients, 295 patients (25.4%) had normal coronary arteries with a patient-level total PV of 0 mm^3. The remaining 867 patients had coronary plaque in segments not included in the current analysis, with a mean patient-level total PV of 127.7 ± 157.1 mm^3.

3.2. Segment based coronary computed tomography angiography findings

Total 9583 segments without any detectable coronary atherosclerotic plaque were identified. The mean length of a coronary segment was 35.0 ± 20.9 mm in baseline CCTA (Table 2). At follow-up CCTA, coronary atherosclerotic plaque with total PV ≥ 1 mm^3 were identified in 939 segments (9.8%) – 9.8% of segments (751 segments from 7674 segments) developed coronary plaque in training set and 9.8% in test set (188 segments from 1721 segments). The mean length of a coronary segment was 35.0 ± 20.9 mm in baseline CCTA and was not different between segments with and without newly developed plaque. In segments with newly developed coronary plaque, the total PV was 15.5 ± 20.5 mm^3 comprising 3.7 ± 8.9 mm^3 of calcified PV and 11.8 ± 17.9 mm^3 of non-calcified PV.

Using the Boruta algorithm, 59 features with the highest score (top 1 rank) were selected from 683 radiomic features with good inter- and intra-observer agreement (both CCC ≥0.85, Supplementary Table 1). In the end, a total of 33 features were finally selected for the modeling after excluding 26 features with no information gain by the XGBoost algorithm. The mean value of the radiomic features included in **Model 2** and **3** is presented in Supplementary Table 2.

3.3. Prediction of the development of new coronary atherosclerotic plaque

Model 1, which included only clinical risk factors, yielded a C-index of 0.701 [95% CI: 0.690–0.712] in the training set and 0.696 [95% CI: 0.667–0.715] in the test set (Table 3, Fig. 2). The C-index of **Model 2**, which was constructed using only the radiomic features extracted from a segment, was not different from that of **Model 1** in both the training set and test sets (C-index [95% CI]: 0.699 [0.688–0.710] and 0.691 [0.667–0.715], respectively, with all $p >$ 00.05 compared to **Model 1**). Continuous NRI and IDI of **Model 1** vs. **Model 2** were both not statistically significant (NRI: −0.086 [95% CI: −0.151 to 0.006] and IDI: −0.086 [95% CI: −0.151 to 0.009], respectively, all $p > 0.05$).

The addition of selected radiomic features to the clinical risk factors significantly improved the C-index of **Model 3** in both the training and test sets (C-index [95% CI]: 0.772 [0.762–0.781] and 0.767 [0.751–0.787], respectively, with $p <$ 00.0001 compared to **Models 1 and 2**). Continuous NRI and IDI of **Model 1** vs. **Model 3** were both positive (0.285 [95% CI: 0.240–0.347] and 0.075 [95% CI: 0.064–0.102], respectively, all $p <$ 00.001), suggesting that **Model 3** is better at predicting the development of a new plaque. The hazard ratio of each radiomic feature in **Model 3** is presented in Supplementary Table 3.

4. Discussion

In the analysis of the PARADIGM registry, the radiomic features significantly improved the prediction of a normal coronary segment that would develop new atherosclerotic coronary artery plaque in near future.

Table 1
Clinical and CCTA characteristics of the study population at baseline.

	Total patient (n = 1162)	Training set (n = 929)	Test set (n = 233)	*P*
Age, years	60.3 ± 9.2	60.2 ± 9.2	60.7 ± 9.1	0.517
Male sex, n (%)	647 (55.7)	515 (55.4)	132 (56.7)	0.795
CCTA interval, years	3.8 ± 1.5	3.8 ± 1.5	3.9 ± 1.6	0.098
Body mass index, kg/m^2	25.2 ± 3.2	25.1 ± 3.1	25.5 ± 3.3	0.138
Hypertension, n (%)	600 (51.6)	486 (52.3)	114 (48.9)	0.394
Diabetes mellitus, n (%)	231 (19.9)	182 (19.6)	49 (21.0)	0.689
Hyperlipidemia, n (%)	420 (36.1)	326 (35.1)	94 (40.3)	0.157
Family history of CAD, n (%)	316 (27.2)	248 (26.7)	68 (29.2)	0.496
Smoking, n (%)	431 (37.1)	339 (36.5)	92 (39.5)	0.441
Total cholesterol, mg/dL	190.0 ± 37.6	189.1 ± 37.9	193.8 ± 36.0	0.082
Low-density lipoprotein, mg/dL	115.6 ± 32.6	114.9 ± 32.8	118.3 ± 31.8	0.148
High-density lipoprotein, mg/dL	51.3 ± 13.2	51.3 ± 3.3	51.6 ± 12.9	0.730
Triglycerides, mg/dL	143.1 ± 82.9	143.4 ± 85.6	141.7 ± 71.3	0.746
Statin, n (%)	625 (53.8)	500 (53.8)	125 (53.7)	0.999
Anti-platelets, n (%)	436 (37.5)	348 (37.5)	88 (37.8)	0.991
Beta-blockers, n (%)	311 (26.8)	241 (25.9)	70 (30.0)	0.237
CCTA characteristics				
Normal CCTA, n (%)	295 (25.4)	238 (25.6)	57 (24.5)	0.781
Total PV in patients with any plaque (mm^3)	127.7 ± 157.1	129.8 ± 160.0	119.5 ± 146.6	0.436

CAD, coronary artery disease; CCTA, coronary computed tomography angiography; PV, plaque volume.

Table 2
CCTA characteristics of segments at baseline and follow-up.

	Total segments (n = 9583)	No plaque at follow-up (n = 8644)	New plaque at follow-up (n = 939)	*P*
CCTA characteristics of segments at baseline				
Segment length, mm	35.0 ± 20.9	35.0 ± 20.8	34.7 ± 22.0	0.750
CCTA characteristics of segments at follow-up				
Segment length, mm	34.9 ± 20.8	34.9 ± 20.7	34.8 ± 21.9	0.835
Total PV, mm^3	0.0	0.0	15.5 ± 20.5	–
Calcified PV, mm^3	0.0	0.0	3.7 ± 8.9	–
Non-calcified PV[a], mm^3	0.0	0.0	11.8 ± 17.9	–
Fibrous PV, mm^3	0.0	0.0	8.2 ± 1.0	–
Fibro-fatty PV, mm^3	0.0	0.0	3.1 ± 7.5	–
Necrotic-core PV, mm^3	0.0	0.0	0.4 ± 2.2	–

CCTA, coronary computed tomography angiography; PV, plaque volume.
[a] Non-calcified PV is the summation of fibrous, fibro-fatty, and necrotic core PV.

Table 3
Multivariate models predicting the development of a coronary plaque within a segment.

	Training set C-index (95% CI)	Test set C-index (95% CI)
Model 1: Clinical risk factors	0.701 (0.690–0.712)	0.696 (0.671–0.725)
Model 2: Radiomic features	0.699 (0.688–0.710)	0.691 (0.667–0.715)
***P* value of Model 1 vs. 2**	0.734	0.728
IDI for Model 1 vs. 2	−0.019 (−0.041 to 0.006), $p = 0.174$	–
NRI for Model 1 vs. 2	−0.086 (−0.151 to 0.009), $p = 0.106$	–
Model 3: Clinical risk factors + radiomics features	0.772 (0.762–0.781)	0.767 (0.751–0.787)
***P* value of Model 1 vs. 3**	<0.0001	<0.0001
IDI for Model 1 vs. 3	0.075 (0.064–0.102), $p < 0.001$	
NRI for Model 1 vs. 3	0.285 (0.240–0.347), $p < 0.001$	
***P* value of Model 2 vs. 3**	<0.0001	<0.0001

CI, confidence interval; IDI, integrated discrimination improvement; NRI, net reclassification improvement.
Adjusted clinical risk factors are age, male sex, body mass index, systolic blood pressure, smoking history, hypertension, diabetes mellitus, family history of coronary artery disease, low-density lipoprotein cholesterol level, medication use including statins, antiplatelets, and beta-blockers, luminal attenuation, and the total plaque volume of the given patient at baseline.

The addition of radiomic features from CCTA images to the conventional risk calculation for atherosclerotic cardiovascular disease using clinical risk factors may help to further refine risk stratification.

Mortality from CAD remains high, and despite improvements in prevention, ACS or cardiac arrest is still the first manifestation of CAD.[1] Studies have repeatedly demonstrated the clinical importance of subclinical atherosclerosis, or nonobstructive CAD.[27,28] The early and accurate identification of patients at higher risk of developing coronary atherosclerosis can guide better preventive care, even in asymptomatic patients without known CAD. Therefore, identifying subgroups of patients who may benefit from repeat CCTA is of paramount importance.

With the latest technological developments, CCTA provides a comprehensive analysis of coronary atherosclerosis. CCTA allows quantification of the total coronary atherosclerotic burden, characterization and hemodynamic assessment of each individual coronary lesion within a patient, and assessment of vascular inflammation.[29–31] CCTA has been shown to identify the culprit lesion in a patient causing the event, and CCTA measures are well associated and may modify future outcomes.[27,30,32]

In this context, studies have been investigated the potential role of CCTA in the low-risk population and the predictive value of normal CCTA.[33–36] As a result, the 2021 multi-society guideline for chest pain suggested a two-year warranty period for CCTA without stenosis or detectable plaques,[37] while more recent studies have suggested a 5–7 years warranty period for normal CCTA.[38] However, despite the large amount of imaging and clinical data from patients with normal CCTA collected over the past decades, the conclusions are still conflicting. The identification of patients at higher risk of developing CAD remains based solely on conventional clinical risk factors, and there has been no way to specifically identify the vessel or segment that will develop new coronary atherosclerotic plaque, while the need for tools to predict plaque development and progression is growing.

In this regard, radiomic analysis of the CCTA image, which extracts more information from images than is visually possible, could be in hand.[8,10] Studies have shown that coronary plaques contain sufficient voxels for radiomic analysis and that radiomic analysis showed better diagnostic performance in assessing coronary plaque vulnerability than conventional CCTA, intravascular ultrasound, and optical coherence tomography.[39–41]

Our study extends the potential role of radiomics in CCTA. By applying radiomics, we aimed to push the limits of CCTA to see if it could characterize visually normal coronary segments that actually contain very early-stage atherosclerotic plaque buds that will later grow to the point of being distinguishable to the naked eye (total PV $\geq$ 1 mm^3), as

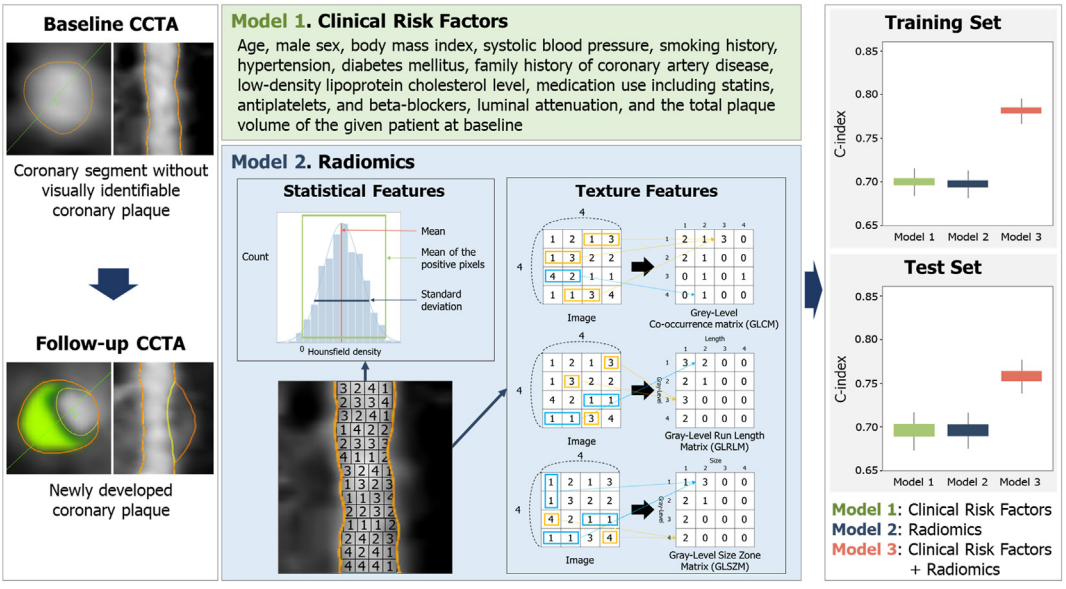

Fig. 2. When models were constructed to identify the coronary segment that will develop new atherosclerotic plaque, models using only radiomic features were not inferior to models constructed using conventional clinical risk factors in both the training and test sets. The addition of both clinical risk factors and radiomic features produced the best results.
CCTA, coronary computed tomography angiography.

well as coronary segments that are more prone to the development of atherosclerosis. In this study, the combination of clinical risk factors and radiomic features significantly improved the predictive power of the models. Importantly, the prognostic value of the model using only radiomic features was not inferior to the model using only traditional clinical risk factors, suggesting that the CCTA image itself may contain information about the patient that is equivalent to clinical features.

Taken together, these results suggest that radiomics can be used as a prescreening tool to aid in cardiovascular risk stratification and identify patients who may benefit from repeat CCTA. Radiomic analysis of CCTA could extend or shorten the warranty period while identifying patients at higher risk of developing CAD, thereby facilitating patient-specific preventive measures and improving the cost-effectiveness of CCTA. Prospective clinical studies are warranted to investigate whether the application of radiomics to "visually" normal CCTA would lead to earlier detection of coronary atherosclerosis and improved prognosis in the primary prevention population, by providing an individually adjusted warranty period of normal CCTA.

4.1. Limitations

Our study has several limitations. Due to the observational nature of the study, selection bias was inevitable because only patients who underwent more than two CCTA scans were eligible for enrollment. High-risk patients who underwent invasive testing or revascularization prior to the second CCTA were excluded from the registry, which may have affected the results. The current analysis excluded patients without a normal segment, making the study population even lower risk.

In addition, the lack of systematic follow-up scans is a critical limitation of the overall analysis. The interval between CCTAs was relatively short, and the differences in scan parameters and vendors between patients and scans may have influenced the results. Therefore, the relevance of the results to high-risk populations with longer follow-up is unknown, and results may be different. However, we adjusted for luminal attenuation, which is associated with quantitative CCTA analysis and radiomics, to minimize the effect of different scan acquisition parameters that were unavoidable in this observational study.[42]

It could be argued that many selected segments already had plaques at baseline CCTA, because the spatial resolution of CCTA is insufficient to determine the presence or absence of plaque and the endpoint is biased. To minimize the potential errors that could be made by the naked eye and currently available CCTA analysis software, we used the commonly used plaque volume threshold of 1 mm^3 to define the identifiable coronary plaque. Furthermore, this study aimed to overcome the spatial resolution limitation of CCTA by applying radiomics. As there are currently no recommendations for the use of serial CCTA,[43] an observational registry such as PARADIGM provides a unique opportunity to capture the development of CAD at its earliest stage. This study demonstrates the potential of radiomics to predict the development of new coronary atherosclerotic plaques from normal coronary segments in a large multinational CCTA registry.

5. Conclusion

The addition of radiomic features to the clinical risk factors significantly improved the prediction of the segment that will develop new atherosclerotic plaques on CCTA by identifying imaging features beyond the human eye. A comprehensive assessment of CCTA using radiomic techniques could help improve risk stratification of patients with potential atherosclerosis.

Formatting of funding sources

This work was supported by the Korea Medical Device Development Fund grant funded by the Korea government (the Ministry of Science and ICT, the Ministry of Trade, Industry and Energy, the Ministry of Health & Welfare, Republic of Korea, the Ministry of Food and Drug Safety) (Project Number: 202016B02). The study was also funded in part by a grant from the Dalio Foundation (New York, NY).

Declaration of competing interest

Dr. Chang receives funding from the Leading Foreign Research Institute Recruitment Program through the National Research Foundation (NRF) of Korea funded by the Ministry of Science and ICT (MSIT) (Grant No. 2012027176). Dr. James K. Min receives funding from GE Healthcare and serves on the scientific advisory board of Arineta and GE Healthcare. Dr. Min also has an equity interest in and is an employee of Cleerly, Inc. The remaining authors have no relevant disclosures.

Appendix A. Supplementary data

Supplementary data to this article can be found online at https://doi.org/10.1016/j.jcct.2024.02.003.

References

1. Tsao CW, Aday AW, Almarzooq ZI, et al. Heart disease and stroke statistics-2022 update: a report from the American Heart association. *Circulation*. 2022;145:e153–e639.
2. Grundy SM, Stone NJ, Bailey AL, et al. 2018 AHA/ACC/AACVPR/AAPA/ABC/ACPM/ADA/AGS/APhA/ASPC/NLA/PCNA guideline on the management of blood cholesterol: executive summary: a report of the American College of Cardiology/American Heart Association task force on clinical practice guidelines. *J Am Coll Cardiol*. 2019;73:3168–3209.
3. Visseren FLJ, Mach F, Smulders YM, et al. 2021 ESC Guidelines on cardiovascular disease prevention in clinical practice. *Eur Heart J*. 2021;42:3227–3337.
4. Lin JS, Evans CV, Johnson E, Redmond N, Coppola EL, Smith N. Nontraditional risk factors in cardiovascular disease risk assessment: updated evidence report and systematic review for the US preventive services task force. *JAMA*. 2018;320:281–297.
5. Knuuti J, Wijns W, Saraste A, et al. 2019 ESC Guidelines for the diagnosis and management of chronic coronary syndromes. *Eur Heart J*. 2020;41:407–477.
6. Leipsic J, Abbara S, Achenbach S, et al. SCCT guidelines for the interpretation and reporting of coronary CT angiography: a report of the Society of Cardiovascular Computed Tomography Guidelines Committee. *J Cardiovasc Comput Tomogr*. 2014;8:342–358.
7. Motoyama S, Ito H, Sarai M, et al. Plaque characterization by coronary computed tomography angiography and the likelihood of acute coronary events in mid-term follow-up. *J Am Coll Cardiol*. 2015;66:337–346.
8. Kolossváry M, De Cecco CN, Feuchtner G, Maurovich-Horvat P. Advanced atherosclerosis imaging by CT: radiomics, machine learning and deep learning. *J Cardiovasc Comput Tomogr*. 2019;13:274–280.
9. Lambin P, Leijenaar RTH, Deist TM, et al. Radiomics: the bridge between medical imaging and personalized medicine. *Nat Rev Clin Oncol*. 2017;14:749–762.
10. Xu P, Xue Y, Schoepf UJ, et al. Radiomics: the next frontier of cardiac computed tomography. *Circ Cardiovasc Imaging*. 2021;14:e011747.
11. Lee SE, Chang HJ, Rizvi A, et al. Rationale and design of the Progression of AtheRosclerotic PlAque DetermIned by Computed TomoGraphic Angiography IMaging (PARADIGM) registry: a comprehensive exploration of plaque progression and its impact on clinical outcomes from a multicenter serial coronary computed tomographic angiography study. *Am Heart J*. 2016;182:72–79.
12. Abbara S, Blanke P, Maroules CD, et al. SCCT guidelines for the performance and acquisition of coronary computed tomographic angiography: a report of the society of cardiovascular computed tomography guidelines committee: endorsed by the north American society for cardiovascular imaging (NASCI). *J Cardiovasc Comput Tomogr*. 2016;10:435–449.
13. Lee SE, Chang HJ, Sung JM, et al. Effects of statins on coronary atherosclerotic plaques: the PARADIGM (progression of AtheRosclerotic PlAque DetermIned by computed TomoGraphic angiography imaging) study. *JACC Cardiovasc Imaging*. 2018;11:1475–1484.
14. Park HB, Lee BK, Shin S, et al. Clinical feasibility of 3D automated coronary atherosclerotic plaque quantification algorithm on coronary computed tomography angiography: comparison with intravascular ultrasound. *Eur Radiol*. 2015;25:3073–3083.
15. Papadopoulou SL, Neefjes LA, Garcia-Garcia HM, et al. Natural history of coronary atherosclerosis by multislice computed tomography. *JACC Cardiovasc Imaging*. 2012;5:S28–S37.
16. Nakazato R, Shalev A, Doh J-H, et al. Aggregate plaque volume by coronary computed tomography angiography is superior and incremental to luminal narrowing for diagnosis of ischemic lesions of intermediate stenosis severity. *J Am Coll Cardiol*. 2013;62:460–467.
17. Lee SE, Park HB, Xuan D, et al. Consistency of quantitative analysis of coronary computed tomography angiography. *J Cardiovasc Comput Tomogr*. 2019;13:48–54.
18. van Griethuysen Jjm, Fedorov A, Parmar C, et al. Computational radiomics system to decode the radiographic phenotype. *Cancer Res*. 2017;77:e104–e107.

19. Choe J, Lee SM, Do KH, et al. Deep learning-based image conversion of CT reconstruction kernels improves radiomics reproducibility for pulmonary nodules or masses. *Radiology*. 2019;292:365–373.
20. Chen Q, Pan T, Wang YN, et al. A coronary CT angiography radiomics model to identify vulnerable plaque and predict cardiovascular events. *Radiology*. 2023;307: e221693.
21. Kursa MB, Rudnicki WR. Feature selection with the Boruta package. *J Stat Software*. 2010;36:1–13.
22. Chen T, He T, Benesty M, et al. Xgboost: extreme gradient boosting. *R package version 0.4-2*. 2015;1:1–4.
23. Al'Aref SJ, Singh G, Choi JW, et al. A boosted ensemble algorithm for determination of plaque stability in high-risk patients on coronary CTA. *JACC Cardiovasc Imaging*. 2020;13:2162–2173.
24. DeLong ER, DeLong DM, Clarke-Pearson DL. Comparing the areas under two or more correlated receiver operating characteristic curves: a nonparametric approach. *Biometrics*. 1988:837–845.
25. Pencina MJ, D'Agostino RB. Overall C as a measure of discrimination in survival analysis: model specific population value and confidence interval estimation. *Stat Med*. 2004;23:2109–2123.
26. Uno H, Tian L, Cai T, Kohane IS, Wei LJ. A unified inference procedure for a class of measures to assess improvement in risk prediction systems with survival data. *Stat Med*. 2013;32:2430–2442.
27. Chang HJ, Lin FY, Lee SE, et al. Coronary atherosclerotic precursors of acute coronary syndromes. *J Am Coll Cardiol*. 2018;71:2511–2522.
28. Kristensen TS, Kofoed KF, Kühl JT, Nielsen WB, Nielsen MB, Kelbæk H. Prognostic implications of nonobstructive coronary plaques in patients with non–ST-segment elevation myocardial infarction: a multidetector computed tomography study. *J Am Coll Cardiol*. 2011;58:502–509.
29. Nørgaard BL, Hjort J, Gaur S, et al. Clinical use of coronary CTA-derived FFR for decision-making in stable CAD. *JACC Cardiovasc Imaging*. 2017;10:541–550.
30. Williams MC, Moss AJ, Dweck M, et al. Coronary artery plaque characteristics associated with adverse outcomes in the SCOT-heart study. *J Am Coll Cardiol*. 2019; 73:291–301.
31. Lee SE, Sung JM, Andreini D, et al. Association between changes in perivascular adipose tissue density and plaque progression. *JACC Cardiovasc Imaging*. 2022;15: 1760–1767.
32. Newby DE, Adamson PD, Berry C, et al. Coronary CT angiography and 5-year risk of myocardial infarction. *N Engl J Med*. 2018;379:924–933.
33. Cho I, Chang HJ, B Óh, et al. Incremental prognostic utility of coronary CT angiography for asymptomatic patients based upon extent and severity of coronary artery calcium: results from the COronary CT Angiography EvaluatioN for Clinical Outcomes InteRnational Multicenter (CONFIRM) study. *Eur Heart J*. 2015;36: 501–508.
34. Halon DA, Lavi I, Barnett-Griness O, et al. Plaque morphology as predictor of late plaque events in patients with asymptomatic type 2 diabetes: a long-term observational study. *JACC Cardiovasc Imaging*. 2019;12:1353–1363.
35. Min JK, Labounty TM, Gomez MJ, et al. Incremental prognostic value of coronary computed tomographic angiography over coronary artery calcium score for risk prediction of major adverse cardiac events in asymptomatic diabetic individuals. *Atherosclerosis*. 2014;232:298–304.
36. Hecht HS. Coronary artery calcium and chest pain: perfect is the enemy of good. *JACC Cardiovasc Imaging*. 2022;15:1758–1759.
37. Gulati M, Levy PD, Mukherjee D, et al. AHA/ACC/ASE/CHEST/SAEM/SCCT/SCMR guideline for the evaluation and diagnosis of chest pain: a report of the American college of cardiology/American Heart association joint committee on clinical practice guidelines, 2021 *Circulation*. 2021;144:e368–e454.
38. Alalawi L, Budoff MJ. Long term prognostic value for a normal CCTA. *J Cardiovasc Comput Tomogr*. 2022;16:531–532.
39. Kolossváry M, Karády J, Szilveszter B, et al. Radiomic features are superior to conventional quantitative computed tomographic metrics to identify coronary plaques with napkin-ring sign. *Circ Cardiovasc Imaging*. 2017;10:e006843.
40. Li XN, Yin WH, Sun Y, et al. Identification of pathology-confirmed vulnerable atherosclerotic lesions by coronary computed tomography angiography using radiomics analysis. *Eur Radiol*. 2022;32:4003–4013.
41. Kolossváry M, Park J, Bang JI, et al. Identification of invasive and radionuclide imaging markers of coronary plaque vulnerability using radiomic analysis of coronary computed tomography angiography. *Eur Heart J Cardiovasc Imaging*. 2019; 20:1250–1258.
42. Takagi H, Leipsic JA, Indraratna P, et al. Association of tube voltage with plaque composition on coronary CT angiography: results from PARADIGM registry. *JACC Cardiovasc Imaging*. 2021;14:2429–2440.
43. Task Force M, Montalescot G, Sechtem U, et al. ESC guidelines on the management of stable coronary artery disease: the Task Force on the management of stable coronary artery disease of the European Society of Cardiology, 2013 *Eur Heart J*. 2013;34: 2949–3003.